Optimal Choice of the Shaft Angle for Involute Gear Hobbing

Carlo Innocenti

Management Summary

With reference to the machining of an involute spur or helical gear by the hobbing process, this paper suggests a new criterion for selecting the position of the hob axis relative to the gear axis. By adhering to the proposed criterion, the hob axis is set at the minimum distance from the gear axis, thus maximizing the depth of the tooth spaces of the gear. The new criterion is operatively implemented by solving a univariate equation, which stems from a new, synthetic analysis of the meshing of crossed-axis, involute gears. A numerical example shows application of the suggested procedure to a case study and compares the optimal hob setting to the customary one.

Introduction

Hobbing of both spur and helical gears is generally done by setting the axes of the gear and the hob at an angle that is the algebraic sum of the pitch helix angles of gear and hob (Refs.1–2). Such a standard way of determining the shaft angle—although conducive to satisfactory results—does not rely on a convincing rationale. Suffice it to say that any referral to pitch helix angles is questionable because the meshing of a hob with the gear being machined does not involve any pure rolling of a pitch cylinder on another pitch cylinder (as would be the case, instead, for the meshing of two gears mounted on parallel-axis shafts).

The possibility of choosing the setting angle of the hob cutter in a non-standard way is mentioned in Reference 3, together with the related implications on the tooth thickness of the hobbed gear for a given gear hob cutting distance. Nevertheless, the technical literature does not seem to have explored this hint, and even more recent contributions on the hobbing process—see, for instance, References 4 and 5—do not question the standard choice of the hob setting angle as the sum of the gear pitch helix angle and of an angle that characterizes the hob.

This paper first revises the kinematics of meshing two crossed-axis, involute helical gears (Refs. 3 and 6), and presents an original, concise relationship for determining the meshing backlash in terms of the gear dimensions, shaft axis distance and shaft axis angle.

Subsequently, the paper narrows the analysis down to the meshing of a gear with a hob. By considering a zero-meshing backlash, the optimal shaft angle for hobbing is determined as the value of the shaft angle that minimizes the shaft axis distance. By adopting this criterion, the depth of the tooth spaces of the gear is maximized, which could be favorable for the contact ratio of a gear pair (undercutting issues are beyond the scope of this work). The paper shows that the value for the optimal shaft angle stems directly from numerically solving a univariate equation.

Embracing the presented method generally leads to shaft angles for hobbing that are very close to those determined by the standard procedure. Even so, the paper highlights the arbitrariness and limitations of the standard procedure for the selection of the hobbing shaft angle. Moreover, it makes available a consistent procedure that is easily employable, despite being more involved than the standard one.

Due to the similarities between the kinematics of the two manufacturing processes, the results reported in the paper for gear hobbing are also applicable to gear grinding when carried out by a threaded grinding wheel.

A numerical example shows application of the presented procedure in a case study and compares the new results to those obtainable by the standard, albeit less-than-optimal procedure.

Contact Between Involute Helicoids

This section and the next one reformulate the basic equations that are instrumental in the analysis of the meshing of a pair of involute helical gears mounted on crossed-axis shafts. Because they involve only the elemental geometric parameters of the gears in mesh, the presented formulas are simpler than those reported in the technical literature, and thus more suited to be algebraically manipulated in the pursuit of this paper's scope. Some of the equations reported in this section stem from specialization of formulas traceable in Reference 7.

The fundamental geometric parameters of an involute helical gear are the radius ρ of the base cylinder, the base helix angle β ($-\pi/2 < \beta < \pi/2$ radians), the number of teeth N, and the angular base thickness φ of a tooth. Aside from N, all of these parameters are shown in Figure 1 with reference to a tooth of a helical gear. (In Figure 1, the involute helicoids are shown as emerging from the base cylinder, irrespective of the actual extent of the tooth flanks. Furthermore, angle β in Figure 1 has to be considered as positive because the base helix angle is right-handed.) The normal base pitch ρ of the gear is the distance between involute helicoids of homologous flanks of adjacent teeth. It is provided by (Ref. 3):

$$p = \frac{2\pi\rho\cos\beta}{N} \tag{1}$$

As soon as the axis of the gear is directed in either way by a unit vector **n**, a tooth flank is a left-hand flank or a right-hand flank according to whether the following quantity is negative or, respectively, positive, as in:

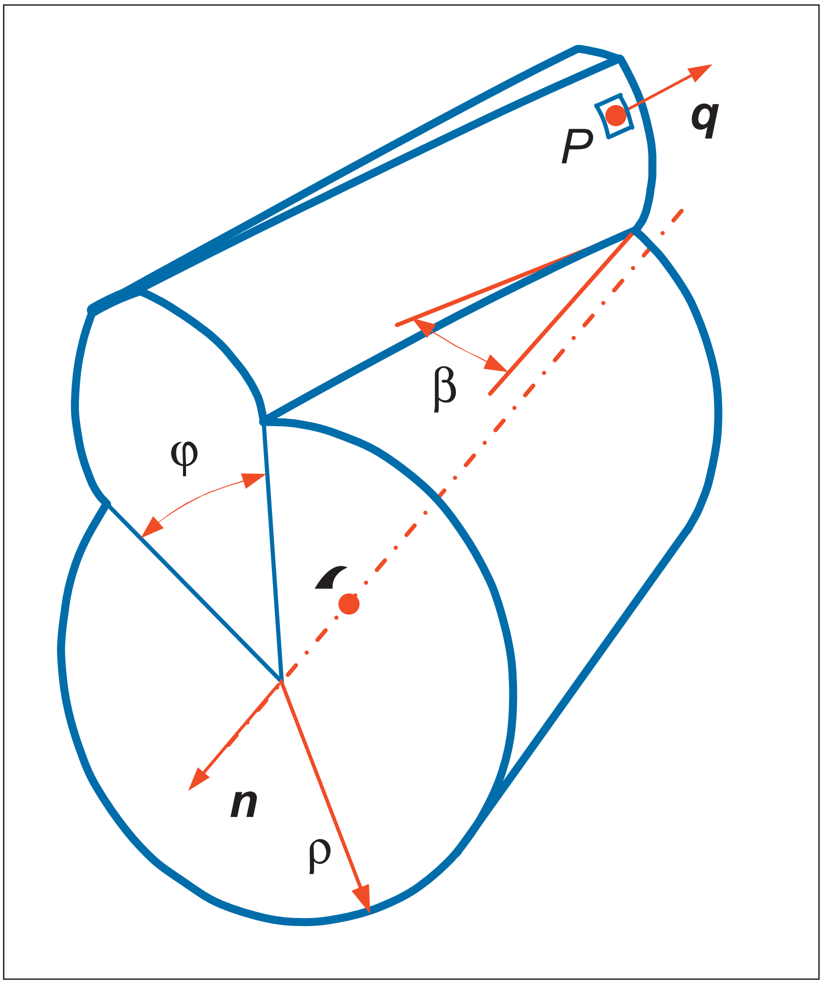

Figure 1—Basic geometric parameters of a helical involute gear.

$$\boldsymbol{q} \times (P - O) \cdot \boldsymbol{n} \tag{2}$$

In Equation 2, (P−O) is the vector from a point O on the gear axis to a point P on the tooth flank, whereas **q** is the outward pointing unit vector orthogonal to the tooth flank at point P.

Two meshing helical involute gears—from here on known as Gear 1 and Gear 2—are now considered. As is known, in order for the gears to mesh, they must have the same normal base pitch. This condition translates into the following equation (see Eq. 1):

$$\frac{N_1}{N_2} = \frac{\rho_1 u_1}{\rho_2 u_2} \tag{3}$$

where quantities u_i ($i = 1,2$) are defined by:

$$u_i = \cos\beta_i \qquad (i = 1, 2) \tag{4}$$

With reference to Figure 2, the distance between the skew gear axes is denoted by a_0. As soon as the axis of Gear 1 is directed in either way by unit vector $\mathbf{n}_1$, unit vector $\mathbf{n}_2$ is so directed as to make a left-hand flank of a tooth of Gear 1 contact a left-hand flank of a tooth of Gear 2. This also implies that if the angular velocity vectors of Gear 1 are positive with respect to $\mathbf{n}_1$, the angular velocity of Gear 2 is negative with respect to $\mathbf{n}_2$).

The common perpendicular to the gear axes intersects the axes themselves at points A_1 and A_2. A fixed reference frame W_1 is now introduced with origin at A_1, x-axis oriented towards A_2, and z- axis parallel to unit vector $\mathbf{n}_1$, with the same direction as $\mathbf{n}_1$. Similarly, another fixed reference frame, W_2, is introduced with origin at A_2, x-axis oriented towards A_1, and z-axis parallel to unit vector $\mathbf{n}_2$, with the same direction. The angle α_0 between the gear axes is defined as the rotation about the x-axis of reference frame W_1 that would make $\mathbf{n}_1$ parallel to $\mathbf{n}_2$. The 4×4 matrix M_0 for transformation of coordinates from W_2 to W_1 is:

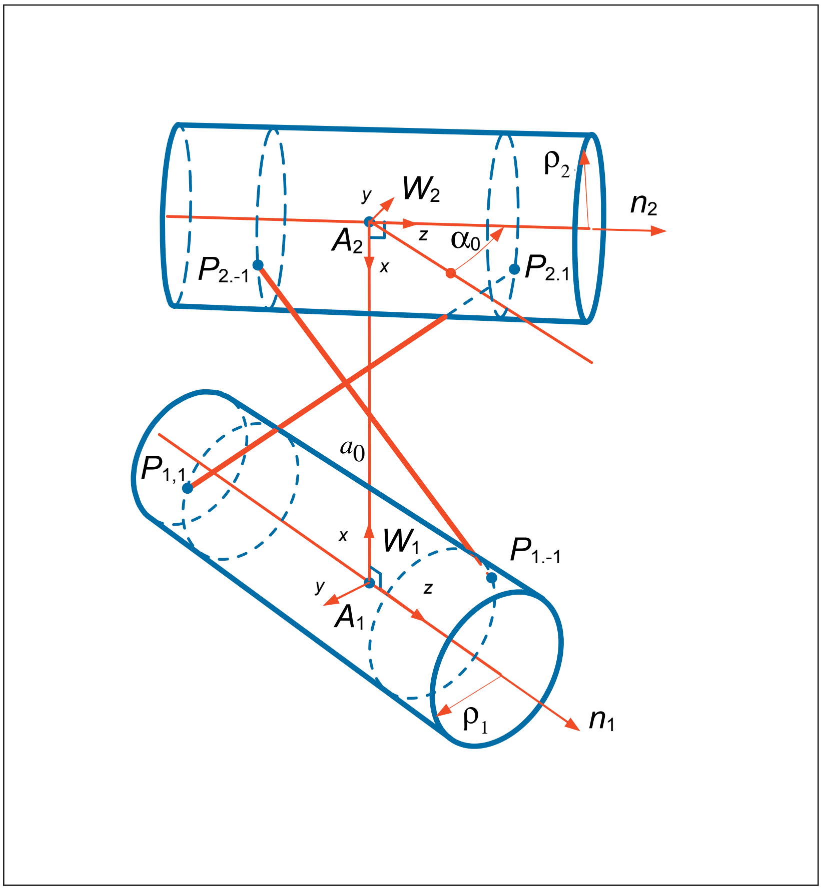

Figure 2—Paths of contact of a crossed-axis helical gearing.

$$M_{i,1} = \begin{bmatrix} c_{i,1} & -s_{i,1} & 0 & 0 \\ s_{i,1} & c_{i,1} & 0 & 0 \\ 0 & 0 & 1 & b_{i,1} \\ 0 & 0 & 0 & 1 \end{bmatrix} \qquad (5)$$

where:

$$u_i = \cos \beta_i \qquad (i = 1, 2) \qquad (6)$$

The point of contact between a right-hand flank of Gear 1 and a right-hand flank of Gear 2 is bound to lie on a straight line that is tangent to the base cylinders of the two gears at points $P_{1,1}$ and $P_{2,1}$. (In this two-index notation, the first index refers to the gear and the second index to the tooth flank—1 for a right-hand flank and –1 for a left-hand flank). The line segment $P_{1,1}$ and $P_{2,1}$ is the path of contact for right-hand flanks.

To determine points $P_{1,1}$ and $P_{2,1}$, together with their mutual distance σ_1, two auxiliary reference frames—$V_{1,1}$ and $V_{2,1}$—are introduced. The origin $B_{i,1}$ of $V_{i,1}$ (i =1, 2) is on the axis of gear i, at the transverse section for gear i that contains point $P_{i,1}$. The z-axis of $V_{i,1}$ has the same orientation and direction as the z-axis of W_i, whereas the x-axis of $V_{i,1}$ is oriented from $B_{i,1}$ to $P_{i,1}$ (Fig. 3). If $\theta_{i,1}$ is the angle of the rotation about the z-axis of W_i, that would make the axes of W_i parallel to the axes of $V_{i,1}$, the 4×4 matrix $M_{i,1}$ for transformation of coordinates from $V_{i,1}$ to W_i is given bv:

$$M_{i,1} = \begin{bmatrix} c_{i,1} & -s_{i,1} & 0 & 0 \\ s_{i,1} & c_{i,1} & 0 & 0 \\ 0 & 0 & 1 & b_{i,1} \\ 0 & 0 & 0 & 1 \end{bmatrix} \qquad (7)$$

where:

$$c_{i,1} = \cos\theta_{i,1}; \qquad s_{i,1} = \sin\theta_{i,1} \qquad (8)$$

and $b_{i,1}$ is the z-coordinate of point $B_{i,1}$ in reference frame W_i.

The homogeneous components in $V_{i,1}$ of the unit vector $\mathbf{e}_{i,1}$ of the contact path $P_{1,1}$ $P_{2,1}$, directed from $P_{i,1}$ to the other extremity of the contact path, is provided by:

$$\mathbf{e}_{i,1}\big|_{Vi,1} = \begin{bmatrix} 0 & -u_i & v_i & 0 \end{bmatrix}^T \qquad (9)$$

where u_i is defined by Equation 4, while v_i is given by:

$$v_i = \sin \beta_i \qquad (i = 1, 2) \qquad (10)$$

Similarly, the homogeneous coordinates of point $P_{i,1}$ with respect to $V_{i,1}$ are:

$$P_{i,1}\big|_{Vi,1} = [\rho_i \quad 0 \quad 0 \quad 1]^T \qquad (11)$$

The ensuing vector conditions:

$$\boldsymbol{e}_{1,1} + \boldsymbol{e}_{2,1} = 0 \qquad (12)$$

$$(P_{2,1} - P_{1,1}) = \sigma_1 \boldsymbol{e}_{1,1} \qquad (13)$$

are conducive to determination of unknowns $\theta_{1,1}$, $\theta_{2,1}$, $b_{1,1}$, $b_{2,1}$, and σ_1. Specifically, Equation 12 imposes the parallelism of the unit vectors $\mathbf{e}_{1,1}$ and $\mathbf{e}_{2,1}$ normal to the right-hand tooth flanks of Gears 1 and 2 at points $P_{1,1}$ and $P_{2,1}$ respectively, whereas Equation 13 calls for unit vector $\mathbf{e}_{1,1}$ to be parallel to contact path $P_{1,1}P_{2,1}$.

To solve Equations 12 and 13, all vectors can be expressed through their components in reference frame W_1. This implies left-multiplying $\mathbf{e}_{1,1}|_{V1,1}$ and $P_{1,1} \mid v_{1,1}$ by matrix $M_{1,1}$, and $\mathbf{e}_{2,1}|_{v2,1}$ and $P_{2,1}| v^{2,1}$ by matrix $M_0M_{2,1}$. If the gear axes are not parallel—i.e., $v_0 \neq 0$—the last two components of Equation 12 linearly provide the ensuing expressions for $c_{1,1}$ and $c_{2,1}$ as:

$$c_{1,1} = -\frac{v_2 + u_0 v_1}{v_0 u_1}; \qquad c_{2,1} = -\frac{v_1 + u_0 v_2}{v_0 u_2} \qquad (14)$$

For a given value of the axis angle α_0—and regardless of the axis distance a_0—the two considered gears can mesh together only if Equation 14 yields cosines of real angles; i.e., only if the following inequality is satisfied:

$$Q \geq 0 \qquad (15)$$

where:

$$Q = v_0^2 - v_1^2 - v_2^2 - 2u_0 v_1 v_2 \qquad (16)$$

By supposing that Equation 15 holds, the first component of Equation 12 provides information on unknowns $s_{1,1}$ and $s_{2,1}$ as:

$$u_1\, s_{1,1} = u_2\, s_{2,1} \qquad (17)$$

As quantities u_1 and u_2 are both positive—they are the cosines of angles lower in magnitude than $\pi/2$—Equation 17 ensures that $s_{1,1}$ and $s_{2,1}$ have the same sign. By also considering that $s_{1,1} = \pm\sqrt{1 - c_{i,1}^2}$, ($i$=1,2), and taking advantage of Equation 14 as well, the ensuing expressions for $s_{1,1}$ and $s_{2,1}$ can be easily found as:

$$s_{1,1} = \lambda \frac{\sqrt{Q}}{v_0\, u_1}; \qquad s_{2,1} = \lambda \frac{\sqrt{Q}}{v_0\, u_2} \qquad (18)$$

In Equation 18, quantity Q is provided by Equation 16, whereas λ is a yet-to-be determined integer whose value is +1 or –1.

An explicit expression of $\theta_{1,1}$ can be obtained through the following trigonometric identity:

$$\tan\frac{\theta_{1,1}}{2} = \frac{1 - c_{1,1}}{s_{1,1}} \qquad (19)$$

With the aid of Equations 14 and 18, Equation 19 yields:

$$\theta_{1,1} = 2\,\lambda \arctan \frac{v_2 + u_0 v_1 + v_0 u_1}{\sqrt{Q}} \qquad (20)$$

The expression of $\theta_{2,1}$ is likewise given by:

$$\theta_{2,1} = 2\,\lambda \arctan \frac{v_1 + u_0 v_2 + v_0 u_2}{\sqrt{Q}} \qquad (21)$$

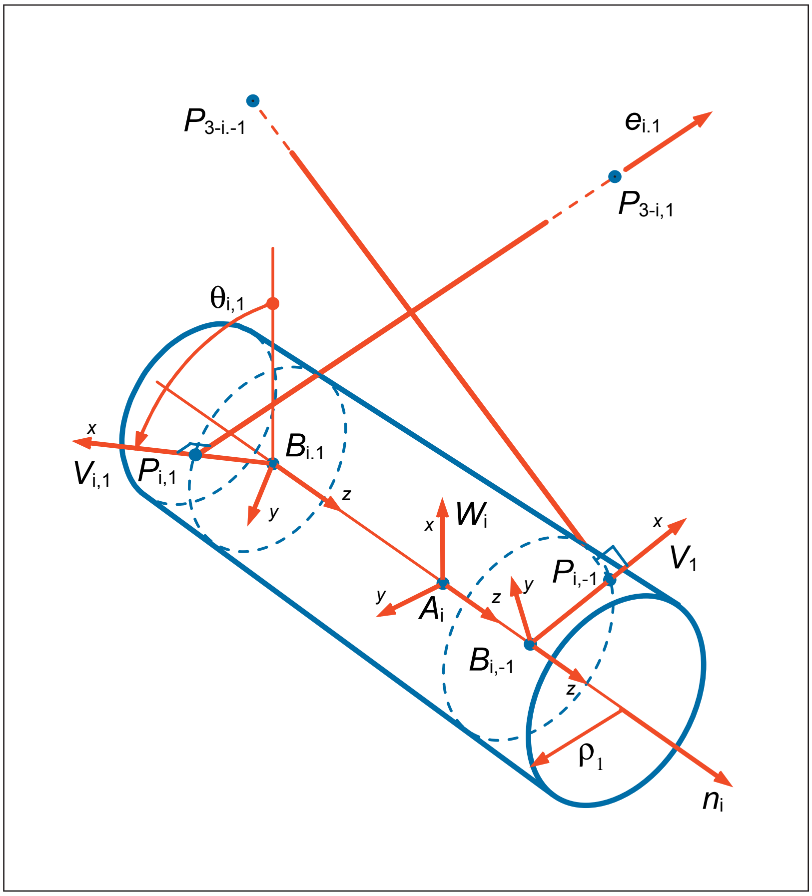

Figure 3—Auxiliary reference frames from gear i (i=1.2).

Equation 13 can now be linearly solved for unknowns $b_{1,1}$, $b_{2,1}$, and σ_1. Specifically, the expression for the length σ_1 of contact path $P_{1,1}$ and $P_{2,1}$ is

$$\sigma_1 = \lambda v_0 \frac{a_0 - \rho_1 c_{1,1} - \rho_2 c_{2,1}}{\sqrt{Q}} \tag{22}$$

Since σ_1 has to be positive, quantity λ is selected as follows:

$$\lambda = \begin{cases} -1 & \text{if} \quad v_0\left(a_0 - \rho_1 c_{1,1} - \rho_2 c_{2,1}\right) < 0 \\ 1 & \text{if} \quad v_0\left(a_0 - \rho_1 c_{1,1} - \rho_2 c_{2,1}\right) \geq 0 \end{cases} \tag{23}$$

Thanks to Equation 23, $s_{1,1}$ and $s_{2,1}$ can be determined by Equation 18. By also taking into account Equation 14, angles $\theta_{1,1}$ and $\theta_{2,1}$ can be unambiguously evaluated in the range $[-\pi, \pi]$ radians through Equations 20 and 21. The expressions for $b_{1,1}$ and $b_{2,1}$ stemming from Equation 13 are:

$$b_{1,1} = -\lambda \frac{a_0 u_1 \left(v_1 + u_0 v_2\right) + \rho_1 v_0 \left(u_0 + v_1 v_2\right) + \rho_2 v_0 u_1 u_2}{v_0 u_1 \sqrt{Q}} \tag{24}$$

$$b_{2,1} = -\lambda \frac{a_0 u_2 \left(v_2 + u_0 v_1\right) + \rho_1 v_0 u_1 u_2 + \rho_2 v_0 \left(u_0 + v_1 v_2\right)}{v_0 u_2 \sqrt{Q}} \tag{25}$$

The results obtained for the contact between right-hand tooth flanks can also be exploited to infer information about the contact between left-hand tooth flanks, as in the path of contact $P_{1,-1}$ $P_{2,-1}$. Indeed, the left-hand flanks of both gears turn into right-hand flanks if the directions of the gear axes—as defined by unit vectors $\mathbf{n}_1$ and $\mathbf{n}_2$—are reversed. Thanks to this observation, the following relationships can be straightforwardly derived as:

$$\begin{array}{ll} \theta_{1,-1} = -\theta_{1,1} & \theta_{2,-1} = -\theta_{2,1} \\ b_{1,-1} = -b_{1,1} & b_{2,-1} = -b_{2,1} \\ \multicolumn{2}{c}{\sigma_{-1} = \sigma_1} \end{array} \tag{26}$$

This concludes determination of the loci of points where the involute helicoids of the two considered gears can come into contact.

Crossed Involute Helical Gears in Mesh

By relying on the results reported in the previous section, this section is devoted to determining the gearing backlash through a procedure similar to the one explained in Equation 7.

The gearing backlash H is here defined by:

$$H = N_1 \Delta\gamma_1 = N_2 \Delta\gamma_2 \tag{27}$$

where N_i and $\Delta\gamma i$ are, respectively, the number of teeth and the angular backlash of gear i (i=1,2).

In order to determine the meshing backlash for Gears 1 and 2 revolving about two given axes, the meshing with zero backlash of Gear 1 with a fictitious gear, referred to as Gear 2′ in the sequel, will be considered. The angular base thickness of Gear 2′ is greater than that of Gear 2 by an amount equal to $\Delta\gamma_2$, in turn related to the meshing backlash H of Gears 1 and 2 by Equation 27.

The involute helicoids L_2 and R_2 defining the left-hand and right-hand flanks of a tooth of Gear 2′ are now considered. Together with any other involute, helicoid gears mentioned in this section, L_2 and R_2 are supposed to extend indefinitely, starting from their base cylinders. L_2 is bound to come into contact with the left-hand flank L_1 of a tooth of Gear 1, while R_2 will touch the right-hand flank R_1 of another tooth of Gear 1, adjacent to the previous one. To find the relationship among the dimensions of the two gears and the relative positions of their axes, the following four-step man euver is imagined:

a) the contact point between involute helicoids L_1 and L_2, initially supposed at $P_{1,1}$, is moved to $P_{2,1}$ by suitably rotating both gears about their axes;

b) by further rotating Gears1 and 2′, helicoids R_1 and R_2 are made to go through point $P_{2,1}$;

c) the contact point between R_1 and R_2 is moved from $P_{2,1}$ to $P_{1,1}$;

d) helicoids L_1 and L_2 are made to go through point $P_{1,-1}$, which brings Gears 1 and 2′ to the position they had at the beginning of the first maneuver.

In the first maneuver, Gear 1 is rotated by an angle γ_{1a} given by (see also Ref. 7):

$$\gamma_{1a} = \frac{\sigma_1}{\rho_1 u_1} \tag{28}$$

In the second maneuver, Gear 2′ revolves about its axis by the following angle:

$$\gamma_{2b} = 2\theta_{2,1} + \varphi_2 + \Delta\gamma_2 - 2\frac{b_{2,1} v_2}{\rho_2 u_2} \tag{29}$$

The corresponding rotation angle for Gear 1 is:

$$\gamma_{1b} = -\frac{N_2}{N_1}\gamma_{2b} \tag{30}$$

To execute the third maneuver, Gear 1 has to revolve by the following angle:

$$\gamma_{1b} = -\frac{N_2}{N_1}\gamma_{2b} \tag{31}$$

Finally, the fourth maneuver requires Gear 1 to be rotated by:

$$\gamma_{1d} = -2\theta_{1,1} - \varphi_1 + 2\frac{b_{1,1}\, v_1}{\rho_1\, u_1} + \frac{2\pi}{N_1} \qquad (32)$$

The series of the above-considered four maneuvers does not alter the angular position of Gear 1; hence the following relationship holds:

$$\gamma_{1a} + \gamma_{1b} + \gamma_{1c} + \gamma_{1d} = 0 \qquad (33)$$

By taking into account Equations 1, and 27 through 32, Equation 33 translates into the following condition:

See this page for equation (34)

Replacement into Equation 34 of the expressions for σ_1, $b_{1,\,1}$, and $b_{2,\,1}$—provided by Equations 22, 24 and 25—leads to:

See this page for equation (35)

This is the key condition for determining the meshing backlash H of a pair of involute helical gears mounted on skew axis shafts. Through Equation 35, the meshing backlash is expressed as a function of the gear geometry p, N_1, N_2, φ_1, φ_2; the relative placement of the gear axes, determined by a_0 and α_0, and quantities that are simple and known functions of these parameters: v_0, λ, Q, $\theta_{1,1}$, $\theta_{2,1}$. See also Equations 6, 23, 16, 20 and 21.

As far as the author is aware, this is the first time that the meshing backlash of two crossed-axis, involute gears is expressed in so concise a form.

Optimal Hob Setting

While a cylindrical involute gear with spur or helical teeth is being hobbed, the meshing of the gear with the hob can be considered as the meshing of two cross-axis, involute helical gears with zero backlash. Therefore the equations drawn in the previous two sections can be employed to analyze the kinematics of the hobbing process, provided that quantity H is set to zero.

The gear being cut and the hob—labeled in the sequel as Gears 1 and 2, and in no specific order—have known kinematically relevant dimensions. The parameters of the relative position of the gear axes—the axis distance a_0 and the axis angle α_0—are subject to the ensuing condition (Equation 35):

$$F\left(a_0, \alpha_0\right) = 0 \qquad (36)$$

where:

See this page for equation (37)

Since Equation 36 is the only condition that parameters a_0 and α_0 have to comply with, there exists a simple infinity of possible relative settings of the hob axis with respect to the gear axis. More precisely, any axis setting that satisfies Equation 36 cuts out the flank of the gear teeth from the same set of involute helicoids (here considered as surfaces with indefinite extent). Simply, different choices of a_0 and α_0 that comply with Equation 36 select different patches from the same set of involute helicoids.

The criterion suggested in this paper for choosing the relative position of the axes of gear and hob is the minimization of the axis distance a_0. The rationale of this choice lies in the consequent maximization of the radial extension of the tooth flanks, for a given hob and a prescribed tip diameter of the gear.

The gear hob axis distance a_0 reaches an extreme value when the ensuing condition is satisfied as:

$$\frac{\partial F}{\partial \alpha_0} = 0 \qquad (38)$$

The minimum possible value of a_0, together with the corresponding value for α_0, derive from simultaneously solving Equations 36 and 38.

To take advantage of Equation 38, some partial derivatives have to be computed. On the right- hand side of Equation 37, quantities

$$\frac{4\pi}{p}\left(\sigma_1 + b_{1,1}v_1 + b_{2,1}v_2\right) - N_1\left(\varphi_1 + 2\theta_{1,1}\right) - N_2\left(\varphi_2 + 2\theta_{2,1}\right) + 2\pi = H$$

Equation 34.

$$\frac{4\pi\,\lambda\sqrt{Q}\,a_0}{p\,v_0} - N_1\left(\varphi_1 + 2\theta_{1,1}\right) - N_2\left(\varphi_2 + 2\theta_{2,1}\right) + 2\pi = H$$

Equation 35.

$$F\left(a_0, \alpha_0\right) = \frac{4\pi\,\lambda\sqrt{Q}\,a_0}{p\,v_0} - N_1\left(\varphi_1 + 2\theta_{1,1}\right) - N_2\left(\varphi_2 + 2\theta_{2,1}\right) + 2\pi$$

Equation 37.

$$\frac{2\pi a_0}{p\,v_0}\left[v_1 v_2 + u_0\left(v_1^2 + v_2^2 + u_0 v_1 v_2\right)\right] + N_1\left(v_1 + u_0 v_2\right) + N_2\left(v_2 + u_0 v_1\right) = 0$$

Equation 42.

$$a_0 = -\frac{p\,v_0}{2\pi}\,\frac{N_1\left(v_1 + u_0 v_2\right) + N_2\left(v_2 + u_0 v_1\right)}{v_1 v_2 + u_0\left(v_1^2 + v_2^2 + u_0 v_1 v_2\right)}$$

Equation 43.

$$2\lambda\sqrt{Q}\,\frac{N_1\left(v_1 + u_0 v_2\right) + N_2\left(v_2 + u_0 v_1\right)}{v_1 v_2 + u_0\left(v_1^2 + v_2^2 + u_0 v_1 v_2\right)} + N_1\left(\varphi_1 + 2\theta_{1,1}\right) + N_2\left(\varphi_2 + 2\theta_{2,1}\right) - 2\pi = 0$$

Equation 44.

Q, v_0, $\theta_{1,1}$, and $\theta_{2,1}$ are functions of α_0. Finding the derivatives of Q and v_0 with respect to α_0 poses no hurdles whatsoever. To determine the derivative of $\theta_{1,1}$ with respect to α_0, both sides of the first of Equations 14 are derived with respect to α_0. Following elementary algebraic manipulation, the ensuing condition is obtained:

$$s_{1,1}\frac{d\theta_{1,1}}{d\alpha_0} = -\frac{v_1 + u_0 v_2}{v_0^2\,u_1} \tag{39}$$

Insertion of the expression of Equation 18 for $s_{1,1}$ yields:

$$\frac{d\theta_{1,1}}{d\alpha_0} = -\lambda\frac{v_1 + u_0 v_2}{v_0\sqrt{Q}} \tag{40}$$

The derivative of $\theta_{2,1}$ with respect to α_0 is obtained in a similar way:

$$\frac{d\theta_{2,1}}{d\alpha_0} = -\lambda\frac{v_2 + u_0 v_1}{v_0\sqrt{Q}} \tag{41}$$

With the aid of Equations 40 and 41, Equation 38 can be rewritten as:

See this page for equation (42)

In order to simultaneously solve Equations 36 and 42, the expression of a_0 as a function of α_0 is first linearly obtained from Equation 42:

See this page for equation (43)

and then inserted into Equation 36. The resulting equation contains α_0 as the only unknown:

See this page for equation (44)

In Equation 44, quantities u_0, v_0, Q, $\theta_{1,1}$, and $\theta_{2,1}$ are functions of α_0. Their expressions in terms of α_0 are given by Equations 6, 16, 20 and 21.

A further comment pertains to quantity λ, which appears in Equation 44, both explicitly and implicitly (see Eqs. 20 and 21). Although the value of λ should be obtained by Equation 23, for the case of a hob cutting a gear, the sum of the base cylinder radii ρ_1 and ρ_2 is generally smaller than the axis distance a_0, hence the following inequality is satisfied as:

$$a_0 - \rho_1 c_{1,1} - \rho_2 c_{2,1} > 0 \tag{45}$$

Consequently, in this case, λ can be given the ensuing simplified expression:

$$\lambda = \begin{cases} -1 & \text{if} \quad v_0 < 0 \\ 1 & \text{if} \quad v_0 \geq 0 \end{cases} \tag{46}$$

The hob shaft angle that allows a given hob to cut a given gear at the minimum axis distance is the value of α_0 that satisfies Equation 44. Once this value has been numerically determined, its insertion into Equation 43 straightforwardly yields the corresponding, or minimum, axis distance a_0.

More generally, Equations 44 and 43 can be resorted to whenever it is of interest to find the relative position of the axes of two cylindrical helical gears with involute teeth that have to mesh together—with no backlash—at the minimum axis distance.

Numerical Example

The results presented in the previous section are here applied to determine the setting parameters for the finish-hobbing operation of a given helical involute gear. Two cases will be considered—cutting by a given right-handed hob and cutting by a left-handed hob that is the mirror image of the former. The results obtained in these two cases will be compared to those stemming from the corresponding customary choice of the hob shaft angle.

Let us suppose that the gear to be hob-machined is characterized by the number of teeth N_1 = 17; normal pressure angle ξ_n = 20°; normal module m_n = 5 mm; helix angle at the standard pitch cylinder β_{p1} = 29.5° ; profile shift x_1= 3 mm.

The hobs are double-threaded, i.e., N_2 = 2. They have the same normal pressure angle and normal module as the gear. Moreover, their addendum is 1.25 times the normal module, and the radius of their tip cylinder is R_{e2} = 65 mm. The cylinder coaxial with each hob that intersects the left-hand and right-hand flanks of the hob threads at equally spaced helices has radius $R_{p2} = R_{e2} - 1.25m_n = 58.75$ mm.

As shown hereafter, standard computations lead to the normal base pitch (p), the angular base thickness (φ_1 and φ_2) and base helix angle (β_1 and β_2) of gear (1) and hobs (2), via determination of the transverse module (m_1 and m_2) and the transverse pressure angle (ξ_1 and ξ_2):

$$p = \pi m_n \cos\xi_n = 14.76065717\text{mm} \quad (47)$$

$$m_1 = \frac{m_n}{\cos\beta_{n1}} = 5.744777708 \text{ mm} \quad (48)$$

$$\xi_1 = \tan^{-1}\left(\frac{\tan\ \xi_n}{\cos\ \beta_{p_1}}\right) = 22.69398023 \text{ deg} \quad (49)$$

See this page for equation (50)

See this page for equation (51)

$$m_2 = \frac{2R_{p_2}}{N_2} = 58.75 \text{ mm} \quad (52)$$

$$\beta_{p_2} = \pm\cos^{-1}\left(\frac{m_n}{m_2}\right) = \pm\ 85.11785767 \text{ deg} \quad (53)$$

$$\xi_2 = \tan^{-1}\left(\frac{\tan\ \xi_n}{\cos\ \beta_{p2}}\right) = 76.83910904 \text{ deg} \quad (54)$$

See this page for equation (55)

See this page for equation (56)

$$\varphi_1 = \left(\frac{\pi\ m_1}{2}\ 2x_1 \tan\xi_1\right)\frac{2}{m_1 N_1} + 2\,\text{inv}\ \xi_1 = 0.2803854852 \text{ rad} = 16.06490494 \text{ deg}$$

Equation 50

$$\beta_1 = \tan^{-1}(\tan\beta_{p1}\cos\xi_1) = 27.56320246 \text{ deg}$$

Equation 51

Table 1—Key geometric parameters of gear and hobs.

	Gear	Hobs
π [mm]	14.76065717	14.76065717
N	17	2
α[deg]	16.06490494	426.38980178
a [deg]	27.56320246	±69.43646886

Table 2—Optimal hob settings.

	Left-threaded Hob	Right-threaded Hob
α_0 [deg]	55.84099326	–114.86308717
a_0 [mm]	110.57666813	110.57666813

Table 3—Customary hob settings.

	Left-threaded Hob	Right-threaded Hob
α_0 [deg]	55.61785767	–114.61785767
a_0 [mm]	110.58061052	110.58061052

$$\varphi_2 = \frac{\pi}{N_2} + 2\,\text{inv}\ \xi_2 = 7.441905938 \text{ rad} = 426.38980178 \text{ deg}$$

Equation 55

$$\beta_2 = \tan^{-1}(\tan\beta_{p2}\ \cos\xi_2) = \pm 69.43646886 \text{ deg}$$

Equation 56

The foregoing computations also yield the hob helix angle β_{p2} at the standard pitch cylinder (β_{p2} is the helix angle measured at distance R_{p2} from the hob axis; the positive value of β_{p2} refers to the right-threaded hob).

All parameters relevant to the analysis at hand (i.e., normal base pitch p, numbers of teeth N, angular base thickness φ, and base helix angle β) are listed in Table 1. The substantial number of decimal digits used in reporting both data and results have the only purpose of allowing the reader to accurately trace the computations here summarily described.

By following the procedure explained in the previous section, the optimal hob settings reported in Table 2 have been obtained. It is worth noting that the shaft angle α_0 referred to in Table 2 has the meaning explained in Section 2, which does not always coincide with the meaning assigned to this term by other authors (for instance, the shaft angle Σ defined in Reference 3 is the opposite of the shaft angle α_0 adopted in this paper).

In order to compare the gain attainable by the proposed procedure for determining the hob setting, the shaft angle α0 has been set at its customary value, i.e. $-(\beta_{p1}+\beta_{p2})$, and the corresponding shaft distance a_0 has been computed by solving Equation 36 (now a linear equation in a_0). The results are reported in Table 3.

A comparison of Tables 2 and 3 reveals that the gain obtained by the proposed procedure is marginal to say the least. With reference to the standard hob setting, the optimum hob setting would require a variation of the shaft angle by a fourth of a degree, the result being a decrease of the shaft axis distance by only 0.004 mm.

Similar observations could be made when comparing the optimal and standard hob settings for an involute spur gear.

Conclusions

The paper has suggested a criterion for selecting the hob setting for cutting spur and helical involute gears. Implementing the proposed criterion requires a transcendental equation in only one unknown to be numerically solved.

Although computationally not very demanding, the presented procedure is more complex than the standard one, and conducive to marginally better results. Therefore the effectiveness of the standard procedure practically rests confirmed.

On the other hand, addressing the considered hob setting problem has led to devising a new formulation of the equations governing the meshing of crossed-axis involute gears. These equations, more lean and compact than those published thus far in the technical literature, could find application to other contexts as well.

References

1. Henriot, G. *Traité Théorique et Pratique des Engranages. Fabrication, Contrôle, Lubrification, Traitement Thermique*. Dunod, Paris, 1972.
2. Townsend, D.P. *Dudley's Gear Handbook*. McGraw Hill, New York, 1992.
3. Colbourne, J.R. *The Geometry of Involute Gears*. Springer Verlag, New York, 1987.
4. Chang, S.L., C.B Tsay and S. Nagata. "A General Mathematical Model for Gears Cut by CNC Hobbing Machines." *ASME Journal of Mechanical Design*, 119, 1997, pp., 108–113.
5. Radzevich, S.P. "About Hob Idle Distance in Gear Hobbing Operation," *ASME Journal of Mechanical Design*, 124, 2002, pp. 772–786.
6. Litvin, F.L., and A. Fuentes. *Gear Geometry and Applied Theory*. Cambridge University Press, 2004.
7. Innocenti, C. "Analysis of Meshing of Beveloid Gears," *Mechanism and Machine Theory*, 32, 1997, pp. 363–373.

A shorter version of this paper was presented at the 2006 ASME International Mechanical Engineering Congress and Exposition, November 5–10, 2006, Chicago, Illinois, USA.